FEASIBILITY OF TWO LOW-COST ORGANIC SUBSTRATES FOR INDUCING DENITRIFICATION IN GROUNDWATER

Alba Grau-Martínez[a*], Clara Torrentó[a,b], Raúl Carrey[a], Paula Rodríguez-Escales[c], Cristina Domènech[a], Giorgio Ghiglieri[d,e], Albert Soler[a], Neus Otero[a]

Keywords

Denitrification, multi-isotopic, permeable reactive barrier, monitored artificial recharge, organic substrate, flow-through experiments.

1. Introduction

Nitrate (NO_3^-) contamination of groundwater usually originates from anthropogenic sources (mainly intensive application of fertilisers and animal manure), and is a major environmental problem that affects several regions of the world (Spalding and Exner, 1993). It is not unusual for groundwater nitrate concentrations to exceed the nominal limit of 50 mg L^{-1} for drinking water set by the 98/83/EC European Union Council Directive. High nitrate ingestion can cause methemoglobinaemia in infants and young children (Magee and Barnes, 1956) and may also promote stomach cancer. Although nitrate contamination of aquifers is a serious environmental and health issue, natural denitrification can occur, reducing pollution levels and diminishing the severity of the problem. This process is considered to be the most important reaction that attenuates nitrate in groundwater (Knowles, 1982). Denitrification may be defined as the dissimilatory microbial reduction of NO_3^- to nitrogen gas (N_2) through several intermediate steps (Eq. 1).

$$NO_3^- \rightarrow NO_2^- \rightarrow NO \rightarrow N_2O \rightarrow N_2 \qquad \text{(Eq.1)}$$

Denitrification takes place under anaerobic conditions where bacteria use nitrate as an oxidant for different materials such as organic matter, sulphides and iron minerals. Denitrification can proceed by the action of heterotrophic or autotrophic bacteria, which

oxidise organic or inorganic substrates, respectively (simplified Eq. 2, 3). In both cases, nitrate is first transformed into nitrite (NO_2^-), which is actually more toxic than nitrate (DeBeer et al., 1997), with a maximum concentration in drinking water of 0.46 mg L^{-1} (Directive 98/83/CE). Through successive steps, nitrite is transformed into nitric oxide (NO), which can further be reduced to nitrous oxide (N_2O); both species are considered greenhouse gases. Finally, nitrous oxide is converted to harmless N_2.

$$5CH_2O + 4NO_3^- + 4H^+ \rightarrow 2N_2 + 5CO_2 + 7H_2O \quad \text{(Eq.2)}$$

$$5FeS_2 + 14NO_3^- + 4H^+ \rightarrow 7N_2 + 10SO_4^{2-} + 5Fe^{2+} + 2H_2O \quad \text{(Eq.3)}$$

Under anaerobic conditions, nitrate may also be reduced to ammonium by a process known as dissimilatory nitrate reduction to ammonium (DNRA or ammonification). DNRA is induced by fermentative bacteria, reducing NO_3^- to NO_2^- before a final reduction to NH_4^+ (Tiedje et al., 1982).

The main limitation of natural attenuation of nitrate is the lack or limited availability of electron donors (Knowles, 1982). Furthermore, the presence of inorganic electron donors, such pyrite, is not abundant. Thus, both autotrophic and heterotrophic denitrification processes are usually limited. For this reason, the most common strategy to remediate nitrate contamination from point source discharges has been the addition of an external electron donor into the system in order to enhance the capacity of indigenous denitrifying biomass to reduce nitrate into dinitrogen gas (Leverenz, et al., 2010; Vidal-Gavilan, et al., 2013). For economical, practical and environmental reasons, an organic carbon source is the most common external electron donor added to the system. Organic carbon can be incorporated into the aquifer via active systems such as injection wells (e.g. Vidal-Gavilan et al., 2013) or passive systems such as permeable reactive barriers, PRBs (Gibert et al., 2008; Robertson et al., 2008).

In arid and semi-arid regions, managed aquifer recharge (MAR) is a widely used technique to increase water supplies. Infiltration and artificial recharge are achieved by ponding or flowing water on the soil surface with basins, furrows, ditches or ponds (Bouwer, 2002). Artificial recharge ponds (ARP) require excavation of permeable terrain

close to the water source (river channel, effluent from a water treatment plant (WTP), etc.). A decantation pond is often included in these systems to improve water quality through deposition of suspended solids. Additionally, in order to improve the quality of both recharged and groundwater, the infiltration ponds can be coupled with a PRB, e.g. an organic reactive layer at the bottom of the pond. The release of organic carbon into the system is expected to enhance endogenous microbiology activity, improving the natural attenuation rate of some target pollutants. A good example of ARP coupled with PRB is located in Sant Vicenç dels Horts (Barcelona, Spain), where the aquifer is recharged by river water. Several studies have shown that the organic reactive layer in this ARP has improved elimination of some organic contaminants (Valhondo et al., 2014). One of the key design parameters in ARP-PRB facilities is the type of material in the reactive layer. This should be effective, economic and easily available. Furthermore, it must be adapted to the socioeconomic circumstances of each country.

In the framework of the project entitled “Water harvesting and Agricultural techniques in Dry lands: an Integrated and Sustainable model in Maghreb Regions” (WADIS-MAR, 2011) a managed artificial recharge system will be installed consisting on ARPs with organic reactive layers in two areas in the Maghreb region (the watersheds of Oued Biskara in Algeria and Oued Oum Zessar in Tunisia) characterised by low soil and aquifer organic matter content, water scarcity, increasing water demand, overexploitation of groundwater resources and high exposure to nitrate contamination. Before implementing the ARPs in the Maghreb region, laboratory feasibility tests were carried out to select the best viable substrate for the reactive layer and to evaluate its capacity to remove nitrate. Several organic substrates, such as compost and softwood, had previously been evaluated for their use in denitrification PRBs (Gibert et al., 2008). In this study, we sought to identify low-cost, easily available and easily handled organic substrates with the capacity to rapidly enhance denitrification in reactive layers in ARPs located in arid and semi-arid regions, where groundwater recharge periods are typically short. In the Maghreb region for example, recharge is mainly due to short, heavy floods caused by

erratic and intense short-term rainfall events. Bearing the above criteria in mind, we selected palm tree leaves and compost, the former because palm trees are typical flora in arid North African regions and the latter to serve for comparison with ARPs in moderate to humid regions such as Sant Vicenç.

Isotopic studies coupled with chemical data are an effective tool to identify and describe denitrification (Aravena and Robertson, 1998). Stable isotopes are usually measured as the ratio between the heavier isotope (e.g.^{15}N) and the lighter isotope (e.g.^{14}N). These ratios are referenced to international standards using delta notation (δ), which is used to express the small variations in isotopic composition that occur and is defined by Eq. 4, where R=^{15}N/^{14}N.

$$\delta^{15}N = \left[{(R_{sample} - R_{std})}/{R_{std}} \right] \times 1000 \qquad \text{(Eq.4)}$$

Furthermore, multi-isotopic studies of the solutes involved in the reactions, such as the δ^{13}C of dissolved inorganic carbon and the δ^{34}S and δ^{18}O of dissolved sulphate, can help determine whether denitrification is promoted by heterotrophic or autotrophic bacteria and identify the existence of secondary processes such as SO_4^{2-} reduction (Mariotti et al., 1988).

The major goal of this study was therefore to assess the denitrification capacity of two substrates for their potential use in ARPs. To this end, laboratory batch and column experiments were performed. The possible adverse effects, such as nitrite accumulation, ammonium formation and sulphate reduction, were also considered and characterised using isotopic and modelling tools. The second goal of this study was to obtain the nitrogen and oxygen isotope fractionations associated with the studied degradation processes to evaluate their potential use as a tool for assessing the efficiency of future enhanced denitrification activities at field scale.

2. Experimental set-up and methods

2.1. Experimental set-up

Batch and flow-through experiments were performed with the two materials tested,

commercial compost from a composting plant located in Moià (Catalonia, NE Spain) and palm tree leaves from the Maghreb region. Both substrates consisted of irregular pieces of organic material between 0.3 and 2 cm in size and were used without any specific pre-treatment. The amount of N and C (%) as well as the $\delta^{15}N$ (‰) and $\delta^{13}C$ (‰) of both substrates was characterised (Table 1).

The groundwater used in all the experiments was from the Llobregat aquifer. This was chosen because it is chemically similar to the Maghreb region groundwater and it significantly facilitated and reduced the cost of the experiment. The groundwater was spiked with $NaNO_3$ in varying amounts (Table 2). All the experiments were performed in a glove box with an argon (batch experiments) or nitrogen (flow-though) atmosphere to avoid the presence of O_2. Experimental oxygen partial pressure in the glove box was maintained between 0.1% and 0.3% O_2, and was continuously monitored by an oxygen partial pressure detector (Sensotran, Gasvisor 6) with an accuracy of ±0.1% O_2.

Four types of batch experiment were performed in sterilised 500 mL glass bottles (Table 3). Commercial compost batch (CCB) and palm tree leaves batch (PTB) experiments were run in triplicate using the selected material and groundwater spiked with 0.80 mM of nitrate previously purged with N_2 for 15 min. A 'sterilised control' experiment (SCB) was carried out adding autoclaved material (palm tree leaves) to autoclaved groundwater which had been previously degassed. In addition, an 'absence control' experiment (ACB) was carried out using only degassed groundwater. Batch experiments with palm tree leaves lasted for 24 hours, whereas those with commercial compost lasted 11 days. In the case of the experiments with compost, bottles were manually shaken once a day. Aqueous samples (5 mL) were periodically collected using sterile syringes. The number of samples was limited to maintain the solution: solid material ratio at 90% of initial value.

The two flow-through experiments were carried out using glass cylindrical columns (35 cm high, 9 cm inner diameter) (Supplementary material, Figure S1). The commercial compost column (CCC) was filled with 1.24 kg of compost mixed with 3.34 kg of clean

silica sand (Panreac®) to increase permeability and prevent flotation of the reactive material. The palm tree column (PTC) was filled with 134 g of palm tree leaves mixed with 3.36 kg of clean silica sand. Thus, total organic C was 40.6 and 18.2 g kg^{-1} for CCC and PTC experiments, respectively. In both experiments, the bottom of the column was filled with silica balls (2 mm Ø) to prevent sediment clogging the outlet. From the results of a bromide tracer test performed just before the start of the experiments, porosity (45% and 28%) and pore volume (0.77 L and 0.52 L) were estimated for the CCC and the PTC experiments, respectively. The input water was spiked with a $NaNO_3$ solution to achieve a known nitrate concentration of between 0.80 mM and 1.61 mM for the CCC experiment and between 2.46 mM and 3.47 mM for the PTC experiment. The columns were filled with water leaving a 4.5 cm free nappe over the sediment to prevent the occurrence of a preferential flow pathway. Both columns operated in downflow mode and the flow rate was controlled by a peristaltic pump (Micropump Reglo Digital 4 channels ISMATEC). In both experiments, two stages were defined separated by a lag period with no flow during which the columns were dried. This lag period was used to simulate a dry period in an artificial recharge set-up. During both stages (I and II), flow rate varied from 0.2 mL min^{-1} to 0.4 mL min^{-1}. The duration and flow rates of each stage are detailed later in this paper for the CCC and PTC experiments, respectively. Both flow-through experiments lasted over 7 months and 76 and 56 samples were collected from the outlet of the CCC and PTC, respectively.

2.2. Analytical methods

Anion (NO_3^-, NO_2^-, Cl^- and SO_4^{2-}) concentrations and isotope ratios ($\delta^{15}N$ and $\delta^{18}O$ of dissolved nitrate) were measured in all the batch experiment samples. Dissolved organic carbon (DOC) was also measured in the first sample of each batch experiment. In the flow-through experiments, anions, cations, ammonium, non-purgeable organic carbon (NPOC) and dissolved inorganic carbon (DIC) were measured, and isotopic data were determined for a subset of samples considered representative according to the

measured concentration of the target analyses. Redox potential (Eh) and pH were measured daily at the column outflow with portable electrodes (WTW-3310). Aliquots of aqueous samples were filtered through 0.2 µm Millipore® filters. Anion concentration was determined by high performance liquid chromatography (HPLC) with a WATERS 515 HPLC pump, IC-PAC anion columns and a WATERS 432 detector. For major cation analysis, samples were acidified with 1% HNO_3^-. Cation concentrations were determined by inductively coupled plasma-optical emission spectrometry (ICP-OES, Perkin-Elmer Optima 3200 RL). Ammonium (NH_4^+) was analysed using ionic chromatography (DIONEX, ICS5000). DOC was measured using organic matter combustion (TOC 500 SHIMADZU), and NPOC was measured by organic matter combustion using a MULTI N/C 3100 Analytik Jena carbon analyser. Periodically, 25 mL of aqueous solution was sampled to measure dissolved inorganic carbon (DIC) by titration (METROHM 702 SM Titrino). Chemical analyses were conducted at the the "Centres Científics i Tecnològics" of the Universitat de Barcelona (CCiT-UB).

The isotopic analyses included the $\delta^{15}N$ and $\delta^{18}O$ of NO_3^-, $\delta^{15}N$ of NH_4^+, $\delta^{34}S$ and $\delta^{18}O$ of SO_4^{2-} and $\delta^{13}C$ of DIC. The $\delta^{15}N$ and $\delta^{18}O$ of dissolved nitrate were determined using a modified cadmium reduction method (Mcllvin and Altabet, 2005; Ryabenko et al., 2009). Briefly, nitrate was converted to nitrite through spongy cadmium reduction and then to nitrous oxide using sodium azide in an acetic acid buffer. Simultaneous $\delta^{15}N$ and $\delta^{18}O$ analysis of the N_2O produced was carried out using a Pre-Con (Thermo Scientific) coupled to a Finnigan MAT-253 Isotope Ratio Mass Spectrometer (IRMS, Thermo Scientific). The $\delta^{15}N$ of NH_4^+ was analysed by the ammonium diffusion method using a Carlo Erba Elemental Analyser (EA) coupled in a continuous flow to a Finnigan Delta C IRMS (Thermo Scientific). For $\delta^{34}S$ and $\delta^{18}O$ analyses, dissolved SO_4^{2-} was precipitated as $BaSO_4$ by adding $BaCl_2 \cdot 2H_2O$ after acidifying the sample with HCl and boiling it to prevent $BaCO_3$ precipitation, following standard methods (Dogramaci et al., 2001). The $\delta^{34}S$ was also analysed with the Carlo Erba EA -Finnigan Delta C IRMS. The $\delta^{18}O$ was analysed in duplicate using a ThermoQuest high temperature conversion elemental

analyser (TC/EA) coupled in continuous flow with a Finnigan MAT Delta C IRMS. For $\delta^{13}C_{DIC,}$ carbonates were converted to CO_2 gas by adding a phosphoric acid solution and the isotope ratio was measured in a Gas-Bench II coupled to a MAT-253 IRMS (Thermo Scientific). The $\delta^{13}C$ and $\delta^{15}N$, as well as total C (%), of the two tested organic substrates were measured using the Carbo Erba EA-Finnigan Delta C IRMS. Isotope ratios were calculated using both international and internal laboratory standards. Notation was expressed in terms of δ relative to the international standards (V-SMOW for $\delta^{18}O$, atmospheric N_2 for $\delta^{15}N$, V-CDT for $\delta^{34}S$ and V-PDB for $\delta^{13}C$). The reproducibility of the samples was ±1‰ for the $\delta^{15}N$ of NO_3^-, ±0.5‰ for the $\delta^{15}N$ of NH_4^+, ±1.5‰ for the $\delta^{18}O$ of NO_3^-, ±0.2‰ for the $\delta^{34}S$ of SO_4^{2-}, ±0.5‰ for the $\delta^{18}O$ of SO_4^{2-}, and ±0.2‰ for the $\delta^{13}C$ of DIC. Samples for isotopic analyses were prepared at the ”Mineralogia Aplicada I Geoquímica de Fluids” laboratory and determined at the “Centres Científics i Tecnològics” of the Universitat de Barcelona (CCiT-UB).

3. Results

Results of the batch experiments are detailed in supplementary material Table S1, and results of the flow through experiments are detailed in Tables S2-S5.

3.1. Batch experiments: chemical data

In the sterilised control (SCB) and absence control (ACB) experiments, nitrate reduction did not occur. Results for commercial compost batch experiments showed complete nitrate consumption in less than 12 days (Fig. 1a). An initial NO_3^- release by the compost of up to 2.58 mM was observed. In the palm tree batch experiment (PTB), complete nitrate reduction was achieved in less than 20 hours with no significant initial NO_3^- release (Fig. 1b). In both batch experiments, transient NO_2^- accumulation was observed. In the CCB experiment, up to 0.1 mM of nitrite was released on the first day, and thereafter nitrite concentration gradually decreased. A similar nitrite trend was observed in the PTB experiment, with a peak of 0.7 mM after 14 hours.

3.2. Flow-through experiments: chemical data

Results for the evolution of NO_3^-, NO_2^-, NH_4^+ and SO_4^{2-} during the flow-through experiments are shown in Figures 2 (CCC) and 3 (PTC). The CCC experiment was characterised by a large initial NO_3^- release (up to 4.3 mM) in the first 4 days of stage I. This NO_3^- was released due to leaching from the compost, similarly to what was observed in the CCB experiment. After that, complete nitrate consumption was achieved. The decrease in NO_3^- concentration was coupled with a slight increase in NO_2^-, which reached values of up to 1.3 mM in the first 7 days. A slight NH_4^+ concentration was detected in the output (values between 0.03 µM and 0.4 mM, Fig. 4a). The concentration of NPOC showed a sharp increase up to 38.4 mM during the first 4 days, followed by a rapid decrease to 0.1 mM (Supplementary material, Table S2). DIC content in the output samples was higher than in the inflow water throughout the experiment, ranging from 6.8 mM to 8.9 mM (Table S2). The SO_4^{2-} concentration in the input water was 1.9 mM, and in the outflow water it ranged from 0.4 mM to 3.8 mM. For most of stage I, outflow SO_4^{2-} concentrations were below inflow concentrations (Fig. 2).

After the 7 week lag period, no NO_3^- leaching from the compost was observed and nitrate concentrations decreased progressively to values below the detection limit (0.002mM). During this stage, no significant NO_2^- accumulation was observed. The outflow concentration values for NH_4^+ and NPOC in stage II remained close to the detection limit (0.03 µM and 8 µM), and SO_4^{2-}concentrations were below inflow concentrations by the end of this stage (after 213 days).

In the PTC experiment, no significant initial NO_3^- and NO_2^- release was observed (Fig. 3). In contrast to the CCC experiment, a sharp increase in NH_4^+ (up to 6.3 mM after 1 day) was detected (Fig. 4b). NPOC concentrations remained stable at between 0.1 mM and 0.2 mM and, in contrast to the CCC experiment, there was no sharp increase at the beginning of the experiment (Supplementary material, Table S4). Output DIC values were lower than input values except on the first day (Table S4). Similarly to the CCC experiment, outflow SO_4^{2-} concentrations were below inflow concentrations for most of

stage I. After the lag period, complete denitrification was again achieved, although small NO_3^- peaks were observed, probably due to flow rate changes. Similarly to the CCC experiment, no significant NO_2^- or NH_4^+ accumulation was observed and outflow sulphate concentrations were below inflow concentrations by the end of stage II (after 173 days). The main difference was a significant initial NPOC release (up to 2.5 mM).

3.3. Isotopic results

In the CCB experiment, an increase of both $\delta^{15}N\text{-}NO_3^-$ (from +9.4‰ to +65.6‰) and $\delta^{18}O\text{-}NO_3^-$ (from +18.6‰ to +52.6‰) was observed as the NO_3^- concentration decreased (Supplementary material, Table S1). In the PTB experiment, the $\delta^{15}N$ of dissolved NO_3^- increased (from +15.40‰ to +32.10‰) as the NO_3^- concentration decreased (Table S1). In the latter experiment, rapid NO_3^- consumption promoted considerable NO_2^- accumulation, hindering the determination of $\delta^{18}O_{NO3}$. A subset of 22 outflow samples from the CCC experiment and 14 samples from the PTC experiment was selected for NO_3^- and NH_4^+ isotopic analyses. In the CCC experiment, the isotopic composition of dissolved NO_3^- showed an increase from +15.0‰ to +61.3‰ for $\delta^{15}N$, and from +10.6‰ to +52.2‰ for $\delta^{18}O$ during the first 10 days of stage I, coinciding with the complete consumption of NO_3^- (Supplementary material, Table S3) . In stage II, $\delta^{15}N$ and $\delta^{18}O$ increased during the two periods of NO_3^- reduction (up to +60.7‰ and +49.8‰, respectively) (Table S3) separated by a NO_3^- rebound linked to an increase in flow rate up to 0.4 mL min^{-1} (from 154 to 165 days). Stage II of the PTC experiment showed a similar trend to that of the CCC experiment, whereby the isotopic composition of dissolved NO_3^- showed an increase from +16.5‰ to +53.2‰ for $\delta^{15}N$, and from +21.4‰ to +62.3‰ for $\delta^{18}O$, coinciding with the complete consumption of NO_3^- (Supplementary material, Table S5). The $\delta^{15}N$ values of dissolved NH_4^+ ranged between +7.1‰ and +11.4‰ in the CCC experiment, whereas a wider range of values was observed in the PTC experiment, from +2.2‰ to +17.9‰ (Fig. 4).

The $\delta^{13}C_{DIC}$ was determined in a subset of 28 samples from stage I of the CCC experiment and 15 samples from both stages of the PTC experiment. The $\delta^{13}C_{DIC}$ values ranged from -13.2‰ to -18.6‰ for the CCC experiment and from -10.3‰ to -18.0‰ (stage I) and from -16.0‰ to -16.9‰ (stage II) for the PTC experiment. A subset of 25 samples from each experiment, with varying SO_4^{2-} concentrations, was analysed to determine the isotopic composition of dissolved SO_4^{2-} ($\delta^{34}S_{SO4}$ and $\delta^{18}O_{SO4}$). In the CCC experiment, the outflow $\delta^{34}S$ and $\delta^{18}O$ values ranged from +7.7‰ to +22.4‰ and from +10.1‰ to +13.6‰, respectively (Supplementary material, Table S3). In the PTC experiment, values ranged from +9.1‰ to +10.6‰ for $\delta^{34}S$, and from +11.2‰ to +11.1‰ for $\delta^{18}O$ (Supplementary material, Table S5)

4. Discussion

4.1. Nitrogen geochemistry and nitrate attenuation

Complete NO_3^- attenuation was achieved in all the experiments. In the column experiments, the CCC experiment showed an initial NO_3^- release, a temporary NO_2^- accumulation, and a slight NH_4^+ increase, whereas in the PTC experiment very low NO_2^- accumulation and a large initial NH_4^+ increase was observed. This increase in NH_4^+ might indicate NH_4^+ leaching from vegetal decomposition, but could also be generated by DNRA. If NH_4^+ was leached from the organic substrates, its isotopic composition should be in agreement with the reactive material (compost/palm leaves). This was observed in the CCC experiment and in the first days of the PTC experiment (Fig. 4). Therefore, it is reasonable to assume that NH_4^+ leaching was the main source of NH_4^+ observed at the beginning of both experiments. However, by the end of stage I of the PTC experiment, $\delta^{15}N_{NH4}$ values were significantly higher (up to +16.2‰), a finding that could not be explained by leaching. Instead, a feasible hypothesis is the occurrence of DNRA. In general terms, DNRA is favoured under higher C to NO_3^- ratios when the electron acceptor (NO_3^-) becomes limiting and the system is rich in labile carbon (Korom et al., 1992). However, the extent of this process was limited, since even assuming that NH_4^+

was derived from DNRA, this would only account for a maximum of 15% of NO_3^- attenuation in the PTC experiment. Therefore, the main nitrate attenuation process in both experiments was denitrification.

The NO_3^- reduction pathway depends on the biomass present in the system, which is controlled by the type of organic carbon available (Nijburg et al., 1998). In addition, Abell et al. (2009) have reported that DNRA bacteria have the capacity to use organic substrates unavailable to denitrifier bacteria. It is reasonable to assume that the differences observed in the two experiments with regard to NH_4^+ generation could be explained by the different organic matter used as electron donor. Palm tree leaves have the capacity to release more NH_4^+ than commercial compost, besides being a labile organic substrate that facilitates NH_4^+ formation through the DNRA process. These results are consistent with the marked differences in DOC values obtained in the first sample of the batch experiments: 150 mg L^{-1} for the PTB and 4 mg L^{-1} for the CCB.

4.2. Denitrification rate and organic C reactivity

In order to quantitatively compare the reactivity of the two organic carbon sources, we developed a kinetic model of the two batch experiments. As the observed NO_2^- concentration in the experiments was high (up to 33.4 mg L^{-1}), the model considered two main processes: 1) the degradation of NO_3^- into NO_2^-, and 2) the degradation of NO_2^- into N_2(g). We tested different kinetics during the modelling process, and found that the best combination was zero order kinetics for the degradation of NO_3^- into NO_2^- (Eq. 5) and first order degradation considering inhibition by NO_3^- for the degradation of nitrite into N_2(g) (Eq. 6).

$$r_{NO_3^-} = -K_1 \quad \text{(Eq.5)}$$

$$r_{NO_2^-} = +QK_1 - K_2[NO_2^-]\left(K_i \Big/ K_i + [NO_3^-]\right) \quad \text{(Eq.6)}$$

where r is the degradation rate of NO_3^- and NO_2^- [$ML^{-3}T^{-1}$], K_1 is the zero degradation constant [$ML^{-3}T^{-1}$], Q is the stoichiometric ratio between nitrate and nitrite (1) [-], K_2 is the first order degradation rate [T^{-1}], and K_i is the inhibition parameter [ML^{-3}]. These results

contrast with those reported in previous studies, where the model that fit best was the Monod kinetic model (e.g. Rodriguez-Escales et al., 2014; Carrey et al., 2014a). Zero order kinetics is achieved when the substrate is not limiting. In this case, since labile organic carbon was continuously released into the system, neither nitrate nor organic carbon was limited. However, the degradation of NO_2^- into $N_2(g)$ was limited by the presence of NO_2^- (first order kinetics with respect to NO_2^-). Both rates were solved numerically considering a time step of 0.5 d in the CCB experiment and 0.01 d in the case of PTB. Figure 5 gives the results of the model considering an initial concentration of NO_3^- of 2.5 mM for CCB and 0.85 mM for PTB and the parameters listed in Table 3. Note that the model did not consider NO_3^- leaching in the CCB experiment, where the initial concentration was the sum of that concentration and the initial one.

Regarding the parameters, it can be observed that the K_1 value was 10 times higher in the PTB experiment than in the CCB experiment (Table 3), resulting in a characteristic time (i.e. the inverse of the reaction rate constant) of 0.5 days for PTB compared to 3.7 days for CCB. For the degradation of NO_2^- into $N_2(g)$, differences in the two parameters (K_2 and K_i) were smaller. As NO_2^- production in the PTB experiment was much faster than in the CCB one, and NO_2^- degradation rates were relatively similar in both experiments, higher NO_2^- accumulation was expected in the PTB experiment (Fig. 5).

Kinetic analysis of the column experiments was based on a N input-output mass balance. The nitrate concentration in the inflow water (plus nitrate initially leached from the compost and ammonium initially leached from the palm tree leaves) was considered as the input of the system, while outflow concentrations of NO_3^-, NO_2^- and NH_4^+ were considered as the output. Any gaseous species such as N_2O or N_2 were not considered because they were not measured. The percentage of N consumption was calculated for each stage of both column experiments as the difference between the input and the output N masses in the system (Supplementary material, Table S6). During stage I, higher N consumption was achieved with the palm tree leaves than with the compost, although similar N consumption percentages were obtained in both cases after the lag

period.

Total nitrate removed during the experiments was 83.7 mmol for the CCC experiment and 140.3 mmol for the PTC experiment, respectively (Table S6). Reactive organic carbon was calculated as the sum of the stoichiometric carbon required to oxidise the observed reduced NO_3^- and reduce the observed consumed SO_4^2. Obtained values (125.3 mmols C for CCC and 231.1 mmols C for PTC) corresponded to 0.8% and 4.4% of the total C in both substrates. Degradable organic C, including the organic carbon leached from the substrates, corresponded to 2.4% and 5.1% of the total C present in the commercial compost and palm tree leaves, respectively. Similar reactive organic C percentages have been obtained in other column experiments using fresh or old organic matter (between 2% and 6%, Abell et al., 2009; Carrey et al., 2013).

Palm tree leaves gave a higher denitrification yield (i.e. amount of nitrate consumed per amount of available C) than commercial compost (6 versus 33 mmol NO_3^- / mol C_{org}), probably because the organic carbon was easily degradable by the bacteria present in the water, enabling them to grow rapidly and produce complete nitrate attenuation in a short period of time.

4.3. Nitrate isotope fractionation

Induced denitrification at field scale may be masked by several processes, such as dispersion, diffusion or dilution (mixing) that could change the NO_3^- concentration in groundwater. The isotopic fractionation of N and O for dissolved NO_3^- obtained in lab-scale experiments may be used in future studies to assess system behaviour in the field and optimise full-scale application. Isotopic fractionation during denitrification can be expressed as a Rayleigh distillation process (Eq. 7), from which the isotopic fractionation factor α can be obtained (Mariotti et al., 1988; Aravena and Robertson, 1998).

$$Ln\left(R_t/R_0\right) = (\alpha - 1) * Ln\left(C_t/C_0\right) \quad \text{(Eq.7)}$$

where C_0 and C_t are the initial and residual nitrate concentrations, respectively (mmol L^{-1}), and R_0 and R_t denote the ratios of heavy versus light isotopes in the initial and residual

isotopic ratios, respectively, which are calculated according to Eq. 8.

$$R = \left[\left(\delta/_{1000}\right) + 1\right] \quad \text{(Eq.8)}$$

where δ is the isotopic composition of $\delta^{15}N$ and $\delta^{18}O$ (‰). The term (α - 1) was calculated from the slope of the regression analysis in double-logarithmic plots [$\ln(R_t/R_0)$] over [$\ln(C_t/C_0)$] according to Eq. 7, and converted to isotopic fractionation (ε_N and ε_O) according to Eq. 9.

$$\varepsilon = 1000 \times (\alpha - 1) \quad \text{(Eq.9)}$$

The Rayleigh equation applies to closed system conditions; therefore, isotopic fractionation is commonly calculated in laboratory experiments where conditions are well constrained, no other sinks affect the nitrate pool and the concentration and isotopic composition of nitrate can be considered exclusively determined by nitrate reduction. In the CCB and CCC experiments, denitrification was the only process consuming NO_3^-. In order to calculate the ε_N and ε_O values, all the samples from both batch and column experiments were plotted together due to the similar trends observed. Figure 6 shows the Rayleigh model for CCC and CCB. Using Eq. 9, isotopic fractionations were calculated as -10.8‰ for ε_N and -9.0‰ for ε_O, with a $\varepsilon_N/\varepsilon_O$ of 1.2. Due to the fast rate of NO_3^- consumption and the transient NO_2^- accumulation in the experiments with palm tree leaves, it was not possible to calculate isotopic fractionation in the batch experiments: calculations were therefore based only on the PTC experiment. Furthermore, as DNRA was detected, the isotopic fractionation obtained was an estimation of the isotope ratio changes for both competing processes. The values obtained were ε_N= -9.9‰ and ε_O= -8.6‰ with a $\varepsilon_N/\varepsilon_O$ of 1.15 (Figure 6).

The ε_N and ε_O values obtained were almost equal when using compost or palm tree leaves as substrates, despite the different nitrate reduction rate and the limited contribution of DNRA in the PTC. With high denitrification rates, some authors have observed lower isotopic fractionation (Mariotti et al., 1988) whereas others have reported higher fractionation (Korom et al., 2012). In the present study, isotopic fractionation did

not show any effect related to changes in the attenuation rate, in agreement with previous laboratory experiments (Carrey et al., 2014b). An overview of isotopic fractionation estimated from several laboratory studies is presented in Table 4.

The ε_N and ε_O values obtained in the present study fell within the range of values reported in the literature. The ε_N values obtained were at the lower end of induced denitrification experiment values (Knöller et al., 2011; Carrey et al., 2014b). In general, autotrophic denitrification or pure culture experiments have obtained higher ε_N values (in absolute terms) (Table 4). With regard to ε_O, some authors have reported an inverse fractionation ($\varepsilon_O > 0‰$) due to ^{16}O loss during reduction of NO_3^- to N_2O (Toyoda et al., 2005). The ε_O calculated in the present study showed normal fractionation within the range of reported values for heterotrophic denitrification.

Recent studies have focused on the $\varepsilon_N/\varepsilon_O$ ratio in order to elucidate different processes affecting isotopic fractionation during nitrate reduction (Granger et al., 2008; Knöller et al., 2011). Factors such as pH, salinity or carbon sources have been reported to show no effect on the $\varepsilon_N/\varepsilon_O$ ratio (Granger et al., 2008; Wunderlich et al., 2012). The incorporation of oxygen isotopes from water into nitrate and nitrite and re-oxidation of nitrite to nitrate have been observed to modify ε_O in field studies. These processes tend to reduce ε_O values, increasing the $\varepsilon_N/\varepsilon_O$ ratio up to 1.8 - 2.0. In denitrification laboratory experiments, a wider range has been observed, from 0.96 (Carrey et al., 2013) to 2.9 (Knöller et al., 2011). Higher values can be achieved when important nitrite accumulation and nitrite re-oxidation is produced (Knöller et al., 2011). The $\varepsilon_N/\varepsilon_O$ ratios obtained in the present experiments were of 1.12 for CCB-CCC and 1.15 for PTC. As palm and compost experiments were performed under anaerobic conditions and nitrite accumulation only lasted for a few days, re-oxidation of nitrite can be ruled out. In addition, due to rapid nitrate reduction and the high isotopic composition of $\delta^{18}O_{NO3}$ (up to +62.3‰), the equilibrium isotope fractionation between water and nitrate can be considered negligible compared to kinetic isotope fractionation during nitrate reduction.

Composition of the microbial community can also affect the $\varepsilon_N/\varepsilon_O$ ratio during

denitrification (Dähnke and Thamdrup, 2016). Deviations in $\varepsilon_N/\varepsilon_O$ ratios can be produced by different enzymes involved in nitrate reduction (Granger et al., 2008). Activity of the periplasmic nitrate reductase (Nap) in denitrifying bacteria resulted in a $\varepsilon_N/\varepsilon_O$ value of ~1.6 (Granger et al., 2008). However, membrane-bound respiratory nitrate reductase (Nar) is more common in classical heterotrophic denitrification and tends to produce $\varepsilon_N/\varepsilon_O$ values of ~1.0 (Granger et al., 2008). The $\varepsilon_N/\varepsilon_O$ ratios obtained in the present experiments were close to 1.0, suggesting a lower influence of periplasmic nitrate reductase, in agreement with nitrate reduction driven by heterotrophic denitrification. As some DNRA was observed in the palm experiment, a higher $\varepsilon_N/\varepsilon_O$ would be expected, since the reduction of nitrate to nitrite by DNRA is considered to be mainly catalysed by Nap complex (Kraft et al., 2011). However, the $\varepsilon_N/\varepsilon_O$ observed in PTC was 1.15, similar to compost (1.12), in agreement with the main role of heterotrophic denitrification in nitrate attenuation. Likewise, the $\varepsilon_N/\varepsilon_O$ ratio in both experiments was close to values obtained in other laboratory experiments involving induced or natural denitrification in freshwater (Granger et al., 2008; Carrey et al., 2013; Carrey et al., 2014b). The published results suggest that denitrification produces ratios of around 1.0 and any deviation can be related to equilibrium isotope fractionation, re-oxidation of nitrite or a different biological pathway of nitrate reduction.

4.4. Sulphate reduction

SO_4^{2-} reduction may be promoted when NO_3^-, Mn and Fe have been entirely consumed but organic carbon is still available. The input water contained Fe and Mn concentrations below the detection limit (2 µM and 0.2 µM, respectively); therefore, once the NO_3^- had been completely consumed, SO_4^{2-} reduction could occur according to the redox sequence in natural systems, since most of the organic matter was still available for degradation. For most of stage I and by the end of stage II in both the CCC and PTC experiments, SO_4^{2-} consumption was observed once all the NO_3^- had been removed. In addition, in both experiments, Eh was close to the values that have been reported to

promote SO_4^{2-} reduction (<-150 mV) Connell and Patrick, 1968). As SO_4^{2-} is reduced, an increase in both $\delta^{34}S_{SO4}$ and $\delta^{18}O_{SO4}$ should be observed (Mizutani and Rafter, 1973), with a higher εS/εO ratio ranging from 2.5 to 4.5 (Mizutani and Rafter, 1969). In the present experiments, both $\delta^{34}S$ and $\delta^{18}O_{SO4}$ increased as the SO_4^{2-} concentration decreased (Supplementary material, Fig.S2), with a higher ratio 6.9 (CCC) and 6.8 (PTC), influenced by an asymptotic behaviour of $\delta^{18}O_{SO4}$ to values of approximately +11‰ for compost and +13‰ for palm tree leaves. During sulphate reduction, oxygen isotope fractionation is controlled by an isotopic equilibration with ambient water (Fritz et al., 1989). Microbial reduction may speed up isotope exchange via cell-internal intermediates so that oxygen isotope fractionation during bacterial sulphate reduction is strongly influenced by an oxygen isotope equilibration with the ambient water (Knöller et al., 2006). The exchange of oxygen from water with sulphate promotes a steady-state value that is determined by the oxygen isotope value of ambient water (Brunner et al., 2005). Consequently, the low εO measured during sulphate reduction suggests an equilibrium with $\delta^{18}O_{H2O}$ that would explain the slightly higher εS/εO observed in these experiments.

5. Conclusions

This study shows that CC and PT have a satisfactory capacity to promote complete denitrification, even after a lag stage without flow, simulating a dry period. However, a potential drawback in the use of these substrates is the initial ammonium release and the slight nitrite accumulation observed suggesting the necessity of a pre-treatment of the material previously to be installed in the MAR system. Overall, the PT gave higher denitrification rate and yield making it suitable for MAR systems in arid and semi-arid climates, where short-term efficient organic substrate is required.

Acknowledgements

This study was financed through the following projects: REMEDIATION (Spanish Government, ref. CGL2014-57215-C4-1-R), MAG (Catalan Government, ref: 2014SGR-

1456) and WADIS-MAR (Water harvesting and Agricultural techniques in Dry lands: an Integrated and Sustainable model in Maghreb Regions, European Commission, ref: ENPI/2011/280-008).

References

Abell, J., Laverman, A.M., Van Cappellen, P., 2009. Bioavailability of organic matter in a freshwater estuarine sediment: long-term degradation experiments with and without nitrate supply. Biogeochemistry 94, 13-28.

Aravena, R., Robertson, W.D., 1998. Use of multiple isotope tracers to evaluate denitrification in ground water: Study of nitrate from a large-flux septic system plume. Ground Water 36, 975-982.

Barford, C.C., Montoya, J.P., Altabet, M.A., Mitchell, R., 1999. Steady-state nitrogen isotope effects of N_2 and N_2O production in Paracoccusdenitrificans. Appl. Environ. Microb. 65, 989-994.

Bouwer, H., 2002. Artificial recharge of groundwater: hydrogeology and engineering. Hydrogeol. J. 10, 121-142.

Brunner, B., Bernasconi, S.M., Kleikemper, J., Schroth, M.H., 2005. A model for oxygen and sulfur isotope fractionation in sulfate during bacterial sulfate reduction processes. Geochim. Cosmochim. Ac. 69, 4773–4785.

Carrey, R., Otero, N., Soler, A., Gomez-Alday, J.J., Ayora, C., 2013. The role of Lower Cretaceous sediments in groundwater nitrate attenuation in central Spain: Column experiments. Appl. Geochem. 32, 142-152.

Carrey, R., Otero, N., Vidal-Gavilan, G., Ayora, C., Soler, A., Gómez-Alday, J.J., 2014a. Induced nitrate attenuation by glucose in groundwater: Flow-through experiment. Chem. Geol. 370, 19-28.

Carrey, R., Rodríguez-Escales, P., Otero, N., Ayora, C., Soler, A., Gómez-Alday, J.J., 2014b. Nitrate attenuation potential of hypersaline lake sediments in central Spain: Flow-through and batch experiments. J. Contam. Hydrol. 164, 323-337.

Connell, W.E., Patrick jr. W.H., 1968. Sulfate reduction in soil: effects of redox potential and pH. Science 159, 86-87.

Dähnke, K., Thamdrup, B., 2016. Isotope fractionation and isotope decoupling during anammox and denitrification in marine sediments. Limnol. Oceanogr. 61, 610-624.

DeBeer, D., Schramm, A., Santegoeds, C.M., Kuhl, M., 1997. A nitrite microsensor for profiling environmental biofilms. Appl. Environ. Microbiol. 63, 973-977.

Directive 98/83/EC. Council Directive 98/83/EC of the European Parliament of the 3 November 1998 on the quality of water intended for human consumption. Off. J. Eur. Communities L 330, of 5.12.1998, 32-54.

Delwiche, C.C., Steyn, P.L., 1970. Nitrogen isotope fractionation in soils and microbial reactions. Environ. Sci. Technol. 4, 929-935.

Dogramaci, S.S., Herczeg, A.L., Schi, S.L., Bone, Y., 2001. Controls on $\delta^{34}S$ and $\delta^{18}O$ of dissolved sulfate in aquifers of the Murray Basin, Australia and their use as indicators of flow processes. Appl. Geochem. 16, 475-488.

Fritz, P., Basharmal, G.M., Drimmie, R.J., Ibsen, J., Qureshi. R.M., 1989. Oxygen isotope exchange between sulphate and water during bacterial reduction of sulphate. Chem. Geol. 79, 99-105.

Gibert, O., Pomierny, S., Rowe, I., Kalin, R.M., 2008. Selection of organic substrates as potential reactive materials for use in a denitrification permeable reactive barrier (PRB). Bioresources Technol. 99, 7587-7596.

Granger, J., Sigman, D.M., Lehmann, M.F., Tortell, P.D., 2008. Nitrogen and oxygen isotope fractionation during dissimilatory nitrate reduction by denitrifying bacteria. Limnol. Oceanogr. 53, 2533-2545.

Grischek, T., Hiscock, K.M., Metschies, T., Dennis, P.F., Nestler, W., 1998. Factors affecting denitrification during infiltration of river water into a sand and gravel aquifer in Saxony, Germany. Water Res.32, 450-460

Hosono, T., Alvarez, K., L., Lin, I.T., Shimada, J., 2015. Nitrogen, carbon, and sulfur isotopic change during heterotrophic (*Pseudomonas aureofaciens*) and autotrophic (*Thiobacillus denitrificans*) denitrification reactions. J. Contam. Hydrol. 183, 72-81.

Knöller, K., Vogt, C., Richnow, H.H., Weise, S.M., 2006. Sulfur and oxygen isotope fractionation during benzene, toluene, ethyl benzene, and xylene degradation by sulfate reducing bacteria. Environ. Sci. Technol. 40, 3879-3885.

Knöller, K., Vogt, C., Haupt, M., Feisthauer, S., Richnow, H.H., 2011. Experimental investigation of nitrogen and oxygen isotope fractionation in nitrate and nitrite during denitrification. Biogeochemistry 103, 371-384.

Knowles, R., 1982. Denitrification. Microbiol. Rev. 46, 43-70.

Korom, S.F., 1992. Natural denitrification in the saturated zone – A review. Water Resour. Research 28, 1657-1668.

Korom, S.F., Schuh, W.M., Tesfay, T., Spencer, E.J., 2012. Aquifer denitrification and in situ mesocosms: Modeling electron donor contributions and measuring rates. J. Hydrol. 432-433, 112-126.

Kraft, B., Strous, M., Tegetmeyer, H.E., 2011. Microbial nitrate respiration – Genes, enzymes and environmental distribution. J. Biotechnol. 155, 104-117.

Leverenz, H.L., Haunschild, K., Hopes, G., Tchobanoglous, G., Darby, J.L., 2010. Anoxic treatment wetlands for denitrification. Ecol. Eng. 36, 1544-1551.

Magee, P.N., Barnes, J.M., 1956. The production of malignant primary hepatic tumours in the rat by feeding dimethylnitrosamine. Br. J. Cancer. 10, 114.

Mariotti, A., Landreau, A., Simon, B., 1988. 15N isotope biogeochemistry and natural denitrification process in groundwater application to the chalk aquifer of northern France. Geochim. Cosmochim. Acta 52, 1869-1878.

McIlvin, M.R., Altabet, M.A., 2005. Chemical conversion of nitrate and nitrite to nitrous oxide for nitrogen and oxygen isotopic analysis in freshwater and seawater. Anal. Chem. 77, 5589-5595.

Mizutani, Y., Rafter, T.A., 1969. Oxygen isotopic composition of sulphates, Part 4. N.Z. J. Sci., 12, 60-68.

Mizutani, Y., Rafter, T.A., 1973. Isotopic behaviour of sulfate oxygen in the bacterial reduction of sulfate. Geochem. J. 6, 183-191.

Nijburg, J.W., Gerards, S., Laanbroek, H.J., 1998. Competition for nitrate and glucose between Pseudomonas fluorescens and Bacillus licheniformis under continuous or fluctuating anoxic conditions. FEMS Microb. Ecol. 26, 345-356.

Robertson, W.D., Vogan, J.L., Lombardo, P.S., 2008. Nitrate removal rates in a 15-year-old permeable reactive barrier treating septic system nitrate. Ground Water Monit. R. 28, 65-72.

Rodríguez-Escales, P., van Breukelen, B.M., Vidal-Gavilan, G., Soler, A., Folch, A., 2014. Integrated modelling of biogeochemical reactions and associated isotope fractionations at batch scale: A tool to monitor enhanced biodenitrification applications. Chem. Geol. 365, 20-29.

Ryabenko, E., Altabet, M.A., Wallace, D.W.R., 2009. Effect of chloride on the chemical conversion of nitrate to nitrous oxide for δ15N analysis. Limnol. Oceanogr. 7, 545-552.

Spalding, R.F., Exner, M.E., 1993. Occurrence of nitrate in groundwater - A review. J. Environ. Qual. 22, 392-402.

Sutka, R.L., Ostrom, N.E., Breznak, P.H., Gandhi, H., Pitt, A.J., Li, F., 2006. Distinguishing nitrous oxide production from nitrification and denitrification on the basis of isotopomer abundances. Appl. Environ. Microbiol. 72, 638-644.

Tiedje, J.M., Sexstone, A.J., Myrold, D.D., Robinson, J.A., 1982. Denitrification: ecological niches, competition and survival. Ant. Van Leeuw. J. Micros, 48, 569-583.

Torrentó, C., Cama, J., Urmeneta, J., Otero, N., Soler, A., 2010. Denitrification of groundwater with pyrite and Thiobacillus denitrificans. Chem. Geol. 278, 80-91.

Torrentó, C., Urmeneta, J., Otero, N., Soler, A., Viñas, M., Cama, J., 2011. Enhanced denitrification in groundwater and sediments from a nitrate-contaminated aquifer after addition of pyrite. Chem. Geol. 287, 90-101.

Toyoda, S., Mutobe, H., Yamagishi, H., Yoshida, N., Tanji, Y., 2005. Fractionation of N2O isotopomers during production by denitrifier. Soil Biol. Biochem. 37, 1535-1545.

Tsushima, K., Ueda, S., Ohno H., Ogura, N., Katase, T., Watanabe, K., 2006. Nitrate decrease with isotopic fractionation in riverside sediment column during infiltration experiment. Water Air Soil Pollut. 174, 47-61.

Valhondo, C., Carrera, J., Ayora, C., Barbieri, M., Noedler, K., Licha, T., Huerta, M., 2014. Behavior of nine selected emerging trace organic contaminants in an artificial recharge system supplemented with a reactive barrier. Environ. Sci. Pollut. R. 21, 11832-11843.

Vidal-Gavilan, G., Folch, A., Otero, N., Solanas, A.M., Soler, A., 2013. Isotope characterization of an in situ biodenitrification pilot-test in a fractured aquifer. Appl. Geochem. 32, 153-163.

Vidal-Gavilan, G., Carrey, R., Solanas, A., Soler, A., 2014. Feeding strategies for groundwater enhanced biodenitrification in an alluvial aquifer: Chemical, microbial and isotope assessment of a 1D flow-through experiment. Sci. Total Environ. 494-495, 241-251.

Wellman, R.P., Cook, F.D., Krouse, H.R., 1968. Nitrogen-15 – microbiological alteration of abundance. Science 161, 269-270.

Wunderlich, A., Meckenstock, R., Einsiedl, F., 2012. Effect of different carbon substrates on nitrate stable isotope fractionation during microbial denitrification. Environ. Sci. Technol. 46, 4861-4868.

Figure captions

Figure 1. Variation in nitrate and nitrite concentrations over time in the batch experiments. (a) CCB and ACB experiments. (b) PTB and SCB experiments. Values and error bars represent the mean and standard deviation, respectively, for the three replicate experiments. Input-NO_3^- concentration is also shown.

Figure 2. NO_3^-, NO_2^-, NH_4^+ and SO_4^{2-} outflow concentrations over time under variable operating conditions for the commercial compost column (CCC) experiment. Nitrate and sulphate content of the inflow water are also shown (continuous and dashed lines, respectively).

Figure 3. Changes in NO_3^-, NO_2^-, NH_4^+ and SO_4^{2-} outflow concentrations over time under variable operating conditions for the palm tree leaves column (PTC) experiment. Nitrate

and sulphate content of the inflow water are also shown (continuous and dashed lines, respectively).

Figure 4. Changes in NH_4^+ concentration and isotopic composition over time in the outflow of both column experiments. (a) Commercial compost column (CCC) and (b) palm tree leaves column (PTC) experiments. In both experiments, dashed lines represent the range of measured values of the $\delta^{15}N$ for each material

Figure 5. Results of the model for the (a) commercial compost batch (CCB) experiment and the (b) palm tree batch (PTB) experiment. Open symbols represent experiment results, whereas dashed and continuous lines represent model results

Figure 6. (a) and (c) $\delta^{15}N$ and (b) and (d) $\delta^{18}O$ of NO_3^- against the natural logarithm of the NO_3^- concentration of CCB-CCC (upper panels) and PTC (lower panels). Slopes of the regression lines represent (α-1), the isotopic fractionation factor for N and O.

Table captions

Table 1. Summary of key parameters of both organic substrates used in the present experiments: commercial compost and palm tree leaves.

Table 2. Experimental conditions of the batch experiments.

Table 3. Kinetic parameters used for modelling batch experiments.

Table 4. Estimated isotopic enrichment factor (εN and εO) obtained in this study and reported in the literature for in situ natural denitrification in laboratory experiments.

Supplementary material

Feasibility of two low-cost organic substrates for inducing denitrification in groundwater

Alba Grau-Martínez[a*], Clara Torrentó[a,b], Raúl Carrey[a], Paula Rodríguez-Escales[c], Cristina Domènech[a], Giorgio Ghiglieri[d,e], Albert Soler[a] , Neus Otero[a]

[a]*Grup de Mineralogia Aplicada i Geoquímica de Fluids, Departament Mineralogia, Petrologia i Geologia Aplicada, SIMGEO UB-CSIC, Facultat de Geologia, Universitat de Barcelona (UB), C/ Martí i Franquès, s/n - 08028 Barcelona, Spain.*

[b]*Centre for Hydrogeology and Geothermics, University of Neuchâtel, Rue Emile-Argand 11, 2000 Neuchâtel, Switzerland.*

[c]*Hydrogeology Group (GHS). Departament of Civil and Environmental Engineering, Universitat Politècnica de Catalunya (UPC), c/Jordi Girona 1-3, 08034 Barcelona, Spain.*

[d]*Department of Chemical and Geological Sciences, University of Cagliari, Via Trentino 51, 09127 Cagliari, Italy.*

[e]*Desertification Research Center-NRD, University of Sassari, Viale Italia 39 – 07100 Sassari, Italy.*

(*) Corresponding author: Alba Grau-Martínez

e-mail: albagrau@ub.edu

Phone: +34 93 403 37 73 Fax: +34 93 402 13 40.

Total number of pages (including cover): 13

Figures: 2

Tables: 6

Figure S1: Flow-through experiments

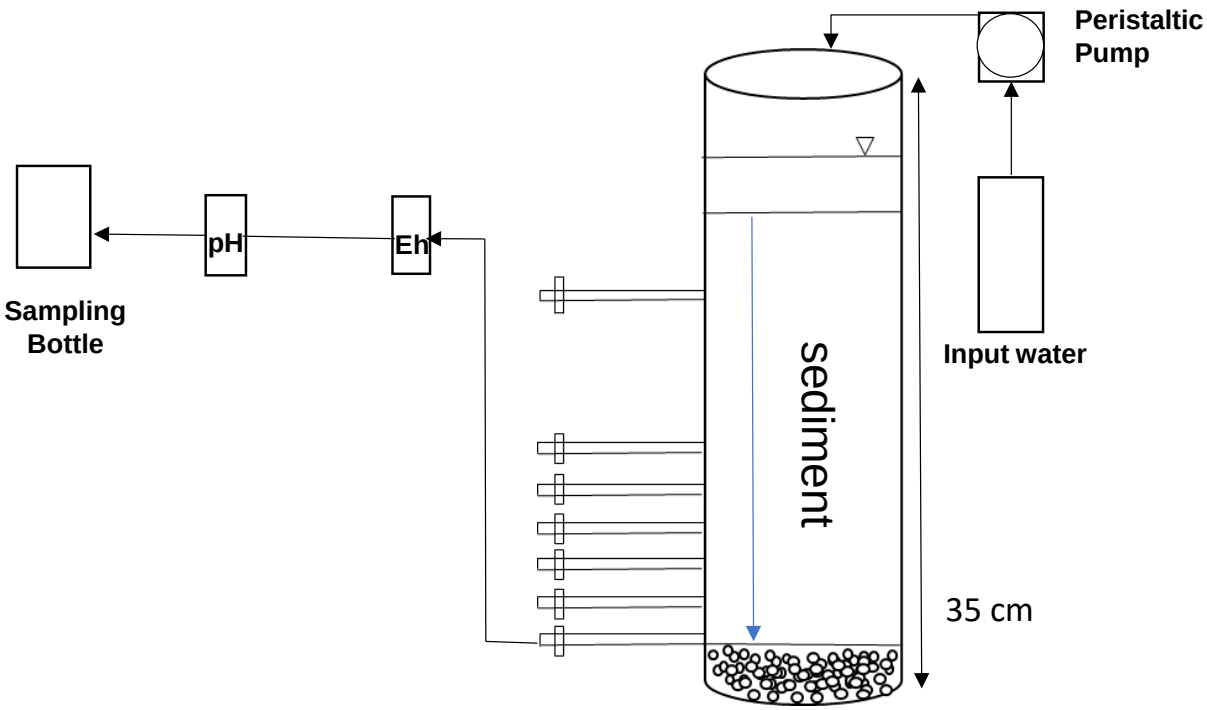

Figure S1. Set-up of the column experiments. Both columns operated in downflow mode.

Figure S6: Sulphate isotope results from the column experiments

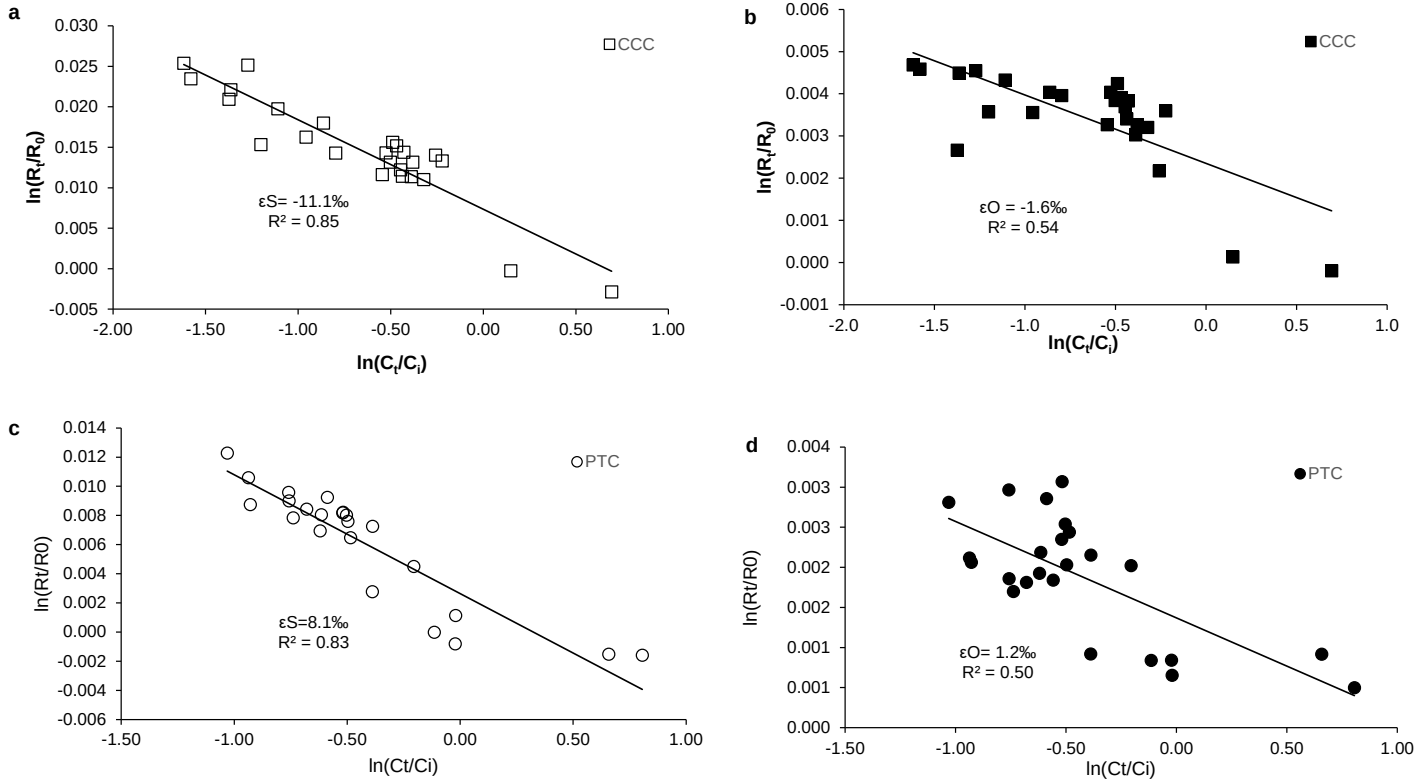

Figure S6. Isotopic results of CCC (upper panels) and PTC (lower panels). (a) and (c) $\ln(R_t/R_0)\delta^{34}S_{SO4}$ vs. $\ln[C_t/C_0]_{SO4}$; (b) and (d) $\ln(R_t/R_0)\ \delta^{18}O_{SO4}$ vs. $\ln[C_t/C_0]_{SO4}$. Values of ε_S and ε_O were obtained from the slope of the regression lines.

Table S1: Results of batch experiments

Table S1. Results of chemical and isotopic characterization of outflow water for batch experiments and input water.

Code	t (d)	avg. NO_3^- (mM)	avg. NO_2^- (mM)	$\delta^{15}N_{NO3}$ (‰)	$\delta^{18}O_{NO3}$ (‰)
CCB					
CB-1	0	2.49	0.01	n.d.	n.d.
CB-2	1	2.17	0.12	+9.39	+18.64
CB-3	3	1.74	0.09	+15.23	+24.37
CB-4	4.9	1.23	0.04	+22.557	+30.38
CB-5	7.1	0.72	0.05	+24.97	+31.99
CB-6	7.3	0.62	0.04	+26.77	+34.26
CB-7	7.9	0.42	0.03	+31.7	+37.19
CB-8	8.2	0.35	0.03	+48.5	+44.3
CB-9	9	0.22	0.02	+65.6	+52.6
CB-10	11	0.05	0.02	n.d.	n.d.
ACB					
ACB-1	0	1.03	0.03		
ACB-2	4.9	1.05	0.02		
ACB-3	11	1.12	0.00		
PTB					
PB-1	0	0.86	0.43	+15.4	+20.5
PB-2	0.02	0.82	0.42	+20.6	+21.5
PB-3	0.44	0.59	0.51	+23.8	+22.5
PB-4	0.58	0.32	0.45	+21.6	+18.8
PB-5	0.67	0.03	0.35	+32.1	+15.0
PB-6	0.75	b.d.l	0.75	n.d.	n.d.
PB-7	0.81	b.d.l	0.81	n.d.	n.d.
PB-8	0.85	b.d.l	0.85	n.d.	n.d.
PB-9	0.92	b.d.l	0.92	n.d.	n.d.
PB-10	0.96	b.d.l	0.96	n.d.	n.d.
PB-11	1	b.d.l	1.00	n.d.	n.d.
PB-12	1.06	b.d.l	1.06	n.d.	n.d.
SCB					
SCB-1	0	1.12	0	n.d.	n.d.
SCB-2	1.06	1.08	0	n.d.	n.d.
Input water					
		0.17	n.d.	+16.5	+21.4

(n.d.:not determined. b.d.l.:below detection limit)

Table S2: Results of commercial compost column experiment.

Table S2. Results of chemical characterization of outflow water for column experiment and input water.

Sample	t (d)	SO_4^{2-} (mM)	NO_3^- (mM)	NO_2^- (mM)	NH_4^+ (mM)	NPOC (mM)	DIC (mM)	pH	Cond (µS/cm)
CCC - Stage I denitrification									
AG-01-Ini	0	1.90	1.04	b.d.l.	0.01	0.14	6.77	7.76	1160
AG-01-01	3	n.d.	n.d.	n.d.	0.07	33.8	7.79	8.17	1395
AG-01-02	4	n.d.	4.33	0.91	0.14	38.44	12.99	8.18	8340
AG-01-03	7	3.83	2.99	1.32	0.16	32.99	16.99	8.5	4290
AG-01-04	8	2.78	1.06	0.13	0.12	26.79	17.21	8.47	3420
AG-01-05	9	3.02	0.44	0.03	0.15	26.81	17.30	8.41	3380
AG-01-06	10	3.38	0.11	0.01	0.19	24.36	18.66	8.32	3160
AG-01-07	11	2.49	b.d.l.	b.d.l.	0.23	24.23	19.02	8.2	3120
AG-01-08	14	2.67	b.d.l.	b.d.l.	0.28	21.25	18.87	7.96	3140
AG-01-09	15	1.88	b.d.l.	b.d.l.	0.26	16.10	16.79	8.35	3700
AG-01-10	16	2.17	b.d.l.	b.d.l.	0.22	15.21	16.08	8.44	3230
AG-01-11	17	2.11	0.01	b.d.l.	0.36	16.24	17.06	8.34	3370
AG-01-12	18	1.64	0.01	b.d.l.	0.33	15.83	17.36	8.05	3490
AG-01-13	21	1.78	0.01	b.d.l.	0.07	15.46	17.58	8.22	3650
AG-01-14	22	0.37	0.01	b.d.l.	0.57	17.48	18.98	8.29	3520
AG-01-15	23	0.50	0.01	b.d.l.	0.53	18.50	17.39	8.22	3060
AG-01-16	24	0.73	b.d.l.	b.d.l.	n.d.	15.79	13.05	8.28	2470
AG-01-17	25	0.93	b.d.l.	b.d.l.	n.d.	14.45	n.d.	8.46	2150
AG-01-18	28	0.61	0.02	b.d.l.	n.d.	11.71	11.06	8.41	1915
AG-01-19	29	0.68	0.02	b.d.l.	n.d.	9.86	n.d.	8.34	1822
AG-01-20	30	0.48	0.01	b.d.l.	n.d.	6.93	11.06	8.24	1797
AG-01-21	31	0.62	b.d.l.	b.d.l.	n.d.	5.05	10.54	8.14	1777
AG-01-22	32	0.71	0.03	b.d.l.	n.d.	0.09	10.52	8.21	1763
AG-01-23	35	0.91	b.d.l.	b.d.l.	n.d.	0.02	9.46	8.13	1726
AG-01-24	36	0.97	0.01	b.d.l.	n.d.	0.02	8.83	8.08	1720
AG-01-25	37	1.30	0.01	b.d.l.	n.d.	0.02	n.d.	8.11	1719
AG-01-26	38	1.27	b.d.l.	b.d.l.	n.d.	0.03	8.69	8.09	1715
AG-01-27	39	1.32	0.02	b.d.l.	n.d.	0.03	8.53	8.92	1711
AG-01-28	42	1.35	0.01	b.d.l.	n.d.	0.05	8.39	8.5	1699
AG-01-29	43	1.38	b.d.l.	b.d.l.	n.d.	0.02	8.23	8.55	n.d.
AG-01-30	44	1.46	b.d.l.	b.d.l.	0.40	0.03	8.44	8.53	1676
AG-01-31	45	1.59	b.d.l.	b.d.l.	0.37	0.05	8.34	8.08	1690
AG-01-32	46	1.42	b.d.l.	b.d.l.	0.41	0.01	8.64	8.13	1732
AG-01-33	49	1.41	b.d.l.	b.d.l.	0.41	0.01	8.80	8.09	1730
AG-01-34	50	1.50	0.01	b.d.l.	0.43	n.d.	8.83	8.14	1742
AG-01-35	51	1.75	0.01	b.d.l.	0.43	0.04	8.61	8.08	1736
AG-01-36	52	1.27	b.d.l.	b.d.l.	0.40	0.05	8.63	7.26	1731
AG-01-37	53	1.46	b.d.l.	b.d.l.	0.44	0.00	8.94	8.22	1746
AG-01-38	59	2.42	0.15	0.02	0.41	0.05	n.d.	n.d.	2190
AG-01-39	64	2.48	1.02	0.02	0.18	0.02	n.d.	n.d.	n.d.
AG-01-40	65	2.60	0.56	0.03	0.30	0.02	n.d.	8.57	n.d.
AG-01-41	66	2.59	0.34	b.d.l.	0.23	0.01	n.d.	9.02	1870
AG-01-42	73	2.38	b.d.l.	b.d.l.	n.d.	n.d.	n.d.	n.d.	1747
Lag period (48 days)									

Sample	t (d)	SO_4^{2-} (mM)	NO_3^- (mM)	NO_2^- (mM)	NH_4^+ (mM)	NPOC (mM)	DIC (mM)	pH	Cond (µS/cm)
CCC - Stage II denitrification									
AG-01'-00	121	1.54	1.53	b.d.l.	0.10	n.d.	5.90	n.d.	n.d.
AG-01'-01	126	1.80	1.04	0.04	n.d.	n.d.	6.33	n.d.	n.d.
AG-01'-02	133	1.87	0.68	0.08	n.d.	0.91	6.72	n.d.	n.d.
AG-01'-03	139	1.76	0.79	0.05	0.10	0.85	n.d.	n.d.	n.d.
AG-01'-04	144	1.71	0.35	0.07	n.d.	n.d.	n.d.	n.d.	n.d.
AG-01'-05	151	1.74	0.20	0.05	n.d.	0.92	n.d.	n.d.	n.d.
AG-01'-06	154	1.54	0.32	0.03	0.10	n.d.	n.d.	n.d.	n.d.
AG-01'-07	157	1.53	0.42	0.01	n.d.	n.d.	n.d.	n.d.	n.d.
AG-01'-08	158	1.60	0.36	0.03	n.d.	n.d.	n.d.	n.d.	n.d.
AG-01'-09	162	1.58	0.57	0.02	n.d.	n.d.	n.d.	n.d.	n.d.
AG-01'-10	164	1.49	1.25	0.00	n.d.	n.d.	n.d.	n.d.	n.d.
AG-01'-11	165	2.27	1.26	0.00	n.d.	n.d.	n.d.	n.d.	n.d.
AG-01'-12	172	1.94	0.89	0.03	n.d.	0.86	n.d.	n.d.	n.d.
AG-01'-13	175	1.92	0.32	0.30	n.d.	0.96	n.d.	n.d.	n.d.
AG-01'-14	176	1.91	0.14	0.25	n.d.	n.d.	n.d.	n.d.	n.d.
AG-01'-15	185	1.94	0.23	0.09	n.d.	n.d.	n.d.	n.d.	n.d.
AG-01'-16	186	1.91	b.d.l.	0.00	n.d.	n.d.	n.d.	n.d.	n.d.
AG-01'-17	190	1.90	b.d.l.	0.00	n.d.	n.d.	n.d.	n.d.	n.d.
AG-01'-18	191	2.56	b.d.l.	0.00	n.d.	n.d.	n.d.	n.d.	n.d.
AG-01'-19	193	2.50	n.d.	0.00	n.d.	n.d.	n.d.	n.d.	n.d.
AG-01'-20	198	2.61	n.d.	0.00	n.d.	0.63	n.d.	n.d.	n.d.
AG-01'-21	199	2.02	b.d.l.	0.00	n.d.	n.d.	n.d.	n.d.	n.d.
AG-01'-22	204	1.91	b.d.l.	0.00	n.d.	0.73	n.d.	n.d.	n.d.
AG-01'-23	206	1.79	0.03	0.00	n.d.	n.d.	n.d.	n.d.	n.d.
AG-01'-24	212	2.05	b.d.l.	0.00	n.d.	n.d.	n.d.	n.d.	n.d.
AG-01'-25	213	1.28	b.d.l.	b.d.l.	n.d.	0.59	n.d.	n.d.	n.d.
AG-01'-26	218	2.05	0.01	b.d.l.	n.d.	n.d.	n.d.	n.d.	n.d.
AG-01'-27	221	2.25	0.01	0.00	n.d.	0.66	n.d.	n.d.	n.d.
AG-01'-28	227	1.56	n.d.	0.00	n.d.	n.d.	n.d.	n.d.	n.d.
AG-01'-29	232	1.57	0.02	0.00	n.d.	n.d.	n.d.	n.d.	n.d.
AG-01'-30	235	1.69	n.d.	0.00	n.d.	n.d.	n.d.	n.d.	n.d.
AG-01'-31	242	1.56	n.d.	0.00	n.d.	n.d.	n.d.	n.d.	n.d.
AG-01'-32	245	1.50	0.01	0.17	n.d.	n.d.	n.d.	n.d.	n.d.
Input Water									
		1.70	0.17	n.d.	n.d.	n.d.	n.d.	7.3	1155

(n.d.:not determined. b.d.l.:below detection limit)

Table S3: Results of commercial compost column experiment.

Table S3. Results of isotopic characterization of outflow water for column experiment and input water.

Sample	$\delta^{15}N_{NO3}$ (‰)	$\delta^{18}O_{NO3}$ (‰)	$\delta^{15}N_{NO2}$ (‰)	$\delta^{18}O_{NO2}$ (‰)	$\delta^{15}N_{NH4}$ (‰)	$\delta^{34}S_{SO4}$ (‰)	$\delta^{18}O_{SO4}$ (‰)	$\delta^{13}C$ (‰)
CCC - Stage I denitrification								
AG-01-Ini	+16.5	+21.4	n.d.	n.d.	n.d.	+10.3	+10.6	-13.2
AG-01-01	n.d.	n.d.	n.d.	n.d.	n.d.	n.d.	n.d.	-21.8
AG-01-02	+15.0	+10.6	-1.3	-5.5	n.d.	n.d.	n.d.	-21.7
AG-01-03	+20.6	+16.3	+6.1	-7.6	n.d.	+7.7	+10.10	-20.6
AG-01-04	+32.9	+28.2	+33.1	-8.8	n.d.	n.d.	n.d.	-20.2
AG-01-05	+38.1	+34.6	n.d.	n.d.	n.d.	n.d.	n.d.	-20.0
AG-01-06	+61.3	+52.2	n.d.	n.d.	n.d.	n.d.	n.d.	-20.4
AG-01-07	n.d.	n.d.	n.d.	n.d.	n.d.	n.d.	n.d.	-20.7
AG-01-08	n.d.	n.d.	n.d.	n.d.	+11	+10.3	+10.4	-20.8
AG-01-09	n.d.	n.d.	n.d.	n.d.	n.d.	n.d.	n.d.	-20.6
AG-01-10	n.d.	n.d.	n.d.	n.d.	n.d.	n.d.	n.d.	-20.7
AG-01-11	n.d.	n.d.	n.d.	n.d.	n.d.	n.d.	n.d.	-20.8
AG-01-12	n.d.	n.d.	n.d.	n.d.	n.d.	n.d.	n.d.	-21.2
AG-01-13	n.d.	n.d.	n.d.	n.d.	n.d.	+24.9	+12.5	-20.9
AG-01-14	n.d.	n.d.	n.d.	n.d.	+7.8	n.d.	n.d.	-21.8
AG-01-15	n.d.	n.d.	n.d.	n.d.	n.d.	+34.6	+14.9	n.d.
AG-01-16	n.d.	n.d.	n.d.	n.d.	n.d.	+26.2	+13.9	n.d.
AG-01-17	n.d.	n.d.	n.d.	n.d.	+7.1	+27.2	+13.9	n.d.
AG-01-18	n.d.	n.d.	n.d.	n.d.	n.d.	+32.0	+13.0	n.d.
AG-01-19	n.d.	n.d.	n.d.	n.d.	n.d.	+36.4	+14.9	-20.1
AG-01-20	n.d.	n.d.	n.d.	n.d.	n.d.	+36.6	+15.0	-20.1
AG-01-21	n.d.	n.d.	n.d.	n.d.	n.d.	+33.2	+14.9	-19.8
AG-01-22	n.d.	n.d.	n.d.	n.d.	n.d.	+30.8	+14.7	-18.7
AG-01-23	n.d.	n.d.	n.d.	n.d.	n.d.	+29.0	+14.4	-19.0
AG-01-24	n.d.	n.d.	n.d.	n.d.	n.d.	+25.1	+14.3	-18.3
AG-01-25	n.d.	n.d.	n.d.	n.d.	n.d.	+24.0	+14.2	-18.2
AG-01-26	n.d.	n.d.	n.d.	n.d.	n.d.	+25.4	+14.4	-17.9
AG-01-27	n.d.	n.d.	n.d.	n.d.	n.d.	+26.5	+14.6	-18.0
AG-01-28	n.d.	n.d.	n.d.	n.d.	n.d.	+26.1	+14.3	-17.8
AG-01-29	n.d.	n.d.	n.d.	n.d.	n.d.	+23.0	+14.0	-17.6
AG-01-30	n.d.	n.d.	n.d.	n.d.	n.d.	+22.2	+13.4	-17.4
AG-01-31	n.d.	n.d.	n.d.	n.d.	n.d.	+21.8	+13.5	n.d.
AG-01-32	n.d.	n.d.	n.d.	n.d.	n.d.	+25.5	+14.2	-18.6
AG-01-33	n.d.	n.d.	n.d.	n.d.	n.d.	+22.2	+13.7	n.d.
AG-01-34	n.d.	n.d.	n.d.	n.d.	+11.4	+24.0	+13.6	n.d.
AG-01-35	n.d.	n.d.	n.d.	n.d.	+11.2	+24.1	+13.9	n.d.
AG-01-36	n.d.	n.d.	n.d.	n.d.	n.d.	+22.4	+13.6	n.d.
AG-01-37	n.d.	n.d.	n.d.	n.d.	n.d.	n.d.	n.d.	n.d.
AG-01-38	n.d.	n.d.	n.d.	n.d.	n.d.	n.d.	n.d.	n.d.
AG-01-39	n.d.	n.d.	n.d.	n.d.	n.d.	n.d.	n.d.	n.d.
AG-01-40	n.d.	n.d.	n.d.	n.d.	n.d.	n.d.	n.d.	n.d.
AG-01-41	n.d.	n.d.	n.d.	n.d.	n.d.	n.d.	n.d.	n.d.
AG-01-42	n.d.	n.d.	n.d.	n.d.	n.d.	n.d.	n.d.	n.d.
Lag period (48 days)								

Sample	$\delta^{15}N_{NO3}$ (‰)	$\delta^{18}O_{NO3}$ (‰)	$\delta^{15}N_{NO2}$ (‰)	$\delta^{18}O_{NO2}$ (‰)	$\delta^{15}N_{NH4}$ (‰)	$\delta^{34}S_{SO4}$ (‰)	$\delta^{18}O_{SO4}$ (‰)	$\delta^{13}C$ (‰)
CCC - Stage II denitrification								
AG-01'-00	+16.5	+21.4	n.d.	n.d.	n.d.	n.d.	n.d.	n.d.
AG-01'-01	+35.4	+35.3	n.d.	n.d.	n.d.	n.d.	n.d.	n.d.
AG-01'-02	+43.1	+45.9	n.d.	n.d.	n.d.	n.d.	n.d.	n.d.
AG-01'-03	+38.2	+36.9	-4.2	+20.7	n.d.	n.d.	n.d.	n.d.
AG-01'-04	+46.2	+50.4	-5.3	+22.6	n.d.	n.d.	n.d.	n.d.
AG-01'-05	+50.9	+41.7	n.d.	n.d.	n.d.	n.d.	n.d.	n.d.
AG-01'-06	+42.9	+38.4	n.d.	n.d.	n.d.	n.d.	n.d.	n.d.
AG-01'-07	+38.6	+38.5	n.d.	n.d.	n.d.	n.d.	n.d.	n.d.
AG-01'-08	+42.6	+36.5	n.d.	n.d.	n.d.	n.d.	n.d.	n.d.
AG-01'-09	+37.6	+29.4	n.d.	n.d.	n.d.	n.d.	n.d.	n.d.
AG-01'-10	+27.8	+21.8	n.d.	n.d.	n.d.	n.d.	n.d.	n.d.
AG-01'-11	+25.7	+20.7	n.d.	n.d.	n.d.	n.d.	n.d.	n.d.
AG-01'-12	+30.9	+31.2	n.d.	n.d.	n.d.	n.d.	n.d.	n.d.
AG-01'-13	+44.9	+39.0	-4.4	+34.8	n.d.	n.d.	n.d.	n.d.
AG-01'-14	+60.7	+49.8	-4.7	+56.18	n.d.	n.d.	n.d.	n.d.
AG-01'-15	+52.6	+40.6	-5.0	+40.16	n.d.	n.d.	n.d.	n.d.
AG-01'-16	n.d.	n.d.	n.d.	n.d.	n.d.	n.d.	n.d.	n.d.
AG-01'-17	n.d.	n.d.	n.d.	n.d.	n.d.	n.d.	n.d.	n.d.
AG-01'-18	n.d.	n.d.	n.d.	n.d.	n.d.	n.d.	n.d.	n.d.
AG-01'-19	n.d.	n.d.	n.d.	n.d.	n.d.	n.d.	n.d.	n.d.
AG-01'-20	n.d.	n.d.	n.d.	n.d.	n.d.	n.d.	n.d.	n.d.
AG-01'-21	n.d.	n.d.	n.d.	n.d.	n.d.	n.d.	n.d.	n.d.
AG-01'-22	n.d.	n.d.	n.d.	n.d.	n.d.	n.d.	n.d.	n.d.
AG-01'-23	n.d.	n.d.	n.d.	n.d.	n.d.	n.d.	n.d.	n.d.
AG-01'-24	n.d.	n.d.	n.d.	n.d.	n.d.	n.d.	n.d.	n.d.
AG-01'-25	n.d.	n.d.	n.d.	n.d.	n.d.	n.d.	n.d.	n.d.
AG-01'-26	n.d.	n.d.	n.d.	n.d.	n.d.	n.d.	n.d.	n.d.
AG-01'-27	n.d.	n.d.	n.d.	n.d.	n.d.	n.d.	n.d.	n.d.
AG-01'-28	n.d.	n.d.	n.d.	n.d.	n.d.	n.d.	n.d.	n.d.
AG-01'-29	n.d.	n.d.	n.d.	n.d.	n.d.	n.d.	n.d.	n.d.
AG-01'-30	n.d.	n.d.	n.d.	n.d.	n.d.	n.d.	n.d.	n.d.
AG-01'-31	n.d.	n.d.	n.d.	n.d.	n.d.	n.d.	n.d.	n.d.
AG-01'-32	n.d.	n.d.	n.d.	n.d.	n.d.	n.d.	n.d.	n.d.
Input Water								
	+16.5	+21.4	n.d.	n.d.	n.d.	+10.3	+10.6	-12.6

(n.d.:not determined)

Table S4: Results of palm tree leave column experiment.

Table S4. Results of chemical characterization of outflow water for column experiment and input water.

Sample	t (d)	SO_4^{2-} (mM)	NO_3^- (mM)	NO_2^- (mM)	NH_4^+ (mM)	NPOC (mM)	DIC (mM)	pH	Cond (µS/cm)
PTC - Stage I denitrification									
AG-02-I	0	2.57	b.d.l.	b.d.l.	4.60	0.33	22.5	6.3	1160
AG-02-01	1	3.24	b.d.l.	b.d.l.	6.29	0.09	26.8	5.6	3210
AG-02-02	4	2.80	b.d.l.	b.d.l.	2.25	0.15	14.4	6.2	3520
AG-02-03	5	2.52	b.d.l.	b.d.l.	1.88	0.19	10.0	6.0	3270
AG-02-04	6	1.75	b.d.l.	b.d.l.	0.91	0.04	4.9	6.7	2780
AG-02-05	7	1.23	0.02	b.d.l.	1.00	0.04	8.1	n.d.	1843
AG-02-06	8	0.92	b.d.l.	b.d.l.	1.44	0.08	11.3	n.d.	n.d.
AG-02-07	11	1.01	0.03	b.d.l.	0.74	b.d.l.	11.3	6.8	n.d.
AG-02-08	12	1.21	0.03	b.d.l.	0.77	0.06	11.4	7.3	1695
AG-02-09	13	1.31	0.03	b.d.l.	0.83	0.11	10.1	7.7	n.d.
AG-02-10	14	1.40	0.03	b.d.l.	0.84	0.09	9.1	n.d.	1710
AG-02-11	15	1.02	0.02	b.d.l.	0.77	0.08	8.5	7.2	1710
AG-02-12	18	1.48	0.02	b.d.l.	0.53	0.01	7.8	7.2	1730
AG-02-13	19	1.39	0.02	b.d.l.	0.60	0.04	8.4	n.d.	1728
AG-02-14	20	1.21	0.02	b.d.l.	0.68	0.08	8.6	7.4	n.d.
AG-02-15	26	1.30	0.02	b.d.l.	0.70	0.14	8.6	7.2	1775
AG-02-16	27	1.39	0.02	b.d.l.	0.46	0.18	8.0	n.d.	1814
AG-02-17	28	1.42	0.02	b.d.l.	0.41	0.03	8.1	7.9	n.d.
AG-02-18	29	1.41	0.01	b.d.l.	0.36	0.10	8.6	7.4	n.d.
AG-02-19	33	1.39	0.01	b.d.l.	0.39	0.09	8.5	7.6	1720
AG-02-20	34	1.59	0.01	b.d.l.	0.39	0.01	8.1	7.4	1728
AG-02-21	35	1.44	b.d.l.	b.d.l.	0.39	0.00	7.8	7.5	1725
AG-02-22	36	1.53	b.d.l.	b.d.l.	0.39	0.05	7.8	7.7	1735
AG-02-23	40	1.84	b.d.l.	b.d.l.	0.38	0.04	n.d.	7.7	1757
AG-02-24	43	1.68	b.d.l.	b.d.l.	0.38	0.07	7.6	n.d.	1730
Lag period (34 days)									

Sample	t (d)	SO_4^{2-} (mM)	NO_3^- (mM)	NO_2^- (mM)	NH_4^+ (mM)	NPOC (mM)	DIC (mM)	pH	Cond (µS/cm)
PTC - Stage II denitrification									
AG-02'-I	77	1.67	1.64	b.d.l.	0.38	2.46	6.2	7.6	2023
AG-02'-01	84	1.68	0.85	0.13	0.39	0.60	6.6	7.9	1900
AG-02'-02	91	1.76	0.38	0.19	0.39	0.50	6.7	n.d.	n.d.
AG-02'-03	98	2.01	0.41	0.10	0.39	0.65	6.7	n.d.	n.d.
AG-02'-04	105	1.94	0.44	0.07	0.40	0.57	6.1	n.d.	n.d.
AG-02'-05	112	1.84	0.95	0.13	n.d.	0.42	n.d.	n.d.	n.d.
AG-02'-06	119	1.74	0.37	0.11	n.d.	n.d.	n.d.	n.d.	n.d.
AG-02'-07	126	1.42	0.11	0.07	0.10	n.d.	n.d.	n.d.	n.d.
AG-02'-08	127	1.38	0.15	0.12	n.d.	n.d.	n.d.	n.d.	n.d.
AG-02'-09	133	1.68	1.00	0.19	n.d.	n.d.	n.d.	n.d.	n.d.
AG-02'-10	139	1.99	0.67	0.19	0.22	n.d.	n.d.	n.d.	n.d.
AG-02'-11	141	1.96	0.34	0.05	n.d.	0.51	n.d.	n.d.	n.d.
AG-02'-12	144	1.91	0.04	0.04	n.d.	0.41	n.d.	n.d.	n.d.
AG-02'-13	147	1.93	0.01	0.01	n.d.	n.d.	n.d.	n.d.	n.d.
AG-02'-14	154	1.89	0.05	0.02	n.d.	0.38	n.d.	n.d.	n.d.
AG-02'-15	155	1.88	0.06	0.03	0.12	n.d.	n.d.	n.d.	n.d.
AG-02'-16	159	1.94	0.13	0.06	n.d.	n.d.	n.d.	n.d.	n.d.
AG-02'-17	160	2.48	0.05	0.04	n.d.	n.d.	n.d.	n.d.	n.d.
AG-02'-18	162	2.32	0.05	0.03	0.10	0.45	n.d.	n.d.	n.d.
AG-02'-19	167	2.28	0.04	0.02	n.d.	n.d.	n.d.	n.d.	n.d.
AG-02'-20	168	1.78	0.04	0.02	n.d.	n.d.	n.d.	n.d.	n.d.
AG-02'-21	173	1.49	0.03	0.01	b.d.l.	0.42	n.d.	n.d.	n.d.
AG-02'-22	174	1.30	0.02	b.d.l.	n.d.	n.d.	n.d.	n.d.	n.d.
AG-02'-23	175	1.59	0.03	b.d.l.	n.d.	n.d.	n.d.	n.d.	n.d.
AG-02'-24	181	1.53	0.02	b.d.l.	n.d.	0.48	n.d.	n.d.	n.d.
AG-02'-25	182	0.60	0.02	0.02	n.d.	n.d.	n.d.	n.d.	n.d.
AG-02'-26	187	1.37	0.06	0.01	n.d.	n.d.	n.d.	n.d.	n.d.
AG-02'-27	190	1.11	0.06	b.d.l.	n.d.	0.69	n.d.	n.d.	n.d.
AG-02'-28	197	0.58	b.d.l.	b.d.l.	n.d.	n.d.	n.d.	n.d.	n.d.
AG-02'-29	200	1.28	b.d.l.	b.d.l.	n.d.	0.42	n.d.	n.d.	n.d.
AG-02'-30	206	1.04	b.d.l.	b.d.l.	n.d.	0.42	n.d.	n.d.	n.d.
AG-02'-31	211	0.86	b.d.l.	b.d.l.	b.d.l.	n.d.	n.d.	n.d.	n.d.
AG-02'-32	216	0.64	b.d.l.	0	n.d.	n.d.	n.d.	n.d.	n.d.
AG-02'-33	222	0.97	b.d.l.	0	n.d.	0.89	n.d.	n.d.	n.d.
Input Water									
		1.70	0.17	n.d.	n.d.	n.d.	n.d.	7.3	1155

(n.d.:not determined. b.d.l.:below detection limit)

Table S5: Results of palm tree leave column experiment.

Table S5. Results of chemical characterization of outflow water for column experiment and input water.

Sample	$\delta^{15}N_{NO3}$ (‰)	$\delta^{18}O_{NO3}$ (‰)	$\delta^{15}N_{NO2}$ (‰)	$\delta^{18}O_{NO2}$ (‰)	$\delta^{15}N_{NH4}$ (‰)	$\delta^{34}S_{SO4}$ (‰)	$\delta^{18}O_{SO4}$ (‰)	$\delta^{13}C$ (‰)
PTC - Stage I denitrification								
AG-02-I	n.d.	n.d.	n.d.	n.d.	n.d.	+9.0	+10.6	-10.3
AG-02-01	n.d.	n.d.	n.d.	n.d.	n.d.	n.d.	+10.8	-10.5
AG-02-02	n.d.	n.d.	n.d.	n.d.	n.d.	+9.1	+11.2	n.d.
AG-02-03	n.d.	n.d.	n.d.	n.d.	+2.9	+9.8	+11.2	n.d.
AG-02-04	n.d.	n.d.	n.d.	n.d.	n.d.	+13.4	+11.2	n.d.
AG-02-05	n.d.	n.d.	n.d.	n.d.	n.d.	+18.5	+12.0	-15.2
AG-02-06	n.d.	n.d.	n.d.	n.d.	+2.2	+23.1	+13.1	n.d.
AG-02-07	n.d.	n.d.	n.d.	n.d.	n.d.	+21.4	+12.4	-17.6
AG-02-08	n.d.	n.d.	n.d.	n.d.	+4.6	+19.7	+12.2	n.d.
AG-02-09	n.d.	n.d.	n.d.	n.d.	n.d.	+19.2	+12.1	n.d.
AG-02-10	n.d.	n.d.	n.d.	n.d.	n.d.	+18.8	+12.5	-16.7
AG-02-11	n.d.	n.d.	n.d.	n.d.	n.d.	+19.5	+12.4	n.d.
AG-02-12	n.d.	n.d.	n.d.	n.d.	n.d.	n.d.	+12.2	-17.7
AG-02-13	n.d.	n.d.	n.d.	n.d.	n.d.	+17.6	+12.2	n.d.
AG-02-14	n.d.	n.d.	n.d.	n.d.	n.d.	+20.3	+13.3	n.d.
AG-02-15	n.d.	n.d.	n.d.	n.d.	+6.0	+20.0	+13.2	-18.9
AG-02-16	n.d.	n.d.	n.d.	n.d.	n.d.	+18.9	+12.7	n.d.
AG-02-17	n.d.	n.d.	n.d.	n.d.	n.d.	+18.3	+12.4	-19.5
AG-02-18	n.d.	n.d.	n.d.	n.d.	n.d.	+18.7	+12.9	n.d.
AG-02-19	n.d.	n.d.	n.d.	n.d.	n.d.	+18.9	+13.4	n.d.
AG-02-20	n.d.	n.d.	n.d.	n.d.	n.d.	+18.0	+12.5	-19.3
AG-02-21	n.d.	n.d.	n.d.	n.d.	n.d.	+17.2	+12.8	n.d.
AG-02-22	n.d.	n.d.	n.d.	n.d.	+16.2	+15.2	+12.3	n.d.
AG-02-23	n.d.	n.d.	n.d.	n.d.	+17.9	+11.7	+11.0	n.d.
AG-02-24	n.d.	n.d.	n.d.	n.d.	+16.8	+10.6	+11.1	-18.0
Lag period (34 days)								

Sample	$\delta^{15}N_{NO3}$ (‰)	$\delta^{18}O_{NO3}$ (‰)	$\delta^{15}N_{NO2}$ (‰)	$\delta^{18}O_{NO2}$ (‰)	$\delta^{15}N_{NH4}$ (‰)	$\delta^{34}S_{SO4}$ (‰)	$\delta^{18}O_{SO4}$ (‰)	$\delta^{13}C$ (‰)
PTC - Stage II denitrification								
AG-02'-I	+16.5	+21.4	n.d.	n.d.	n.d.	n.d.	n.d.	-16.0
AG-02'-01	+21.2	+33.0	+24.5	-5.2	+12.0	n.d.	n.d.	-17.2
AG-02'-02	+26.0	+39.5	+37.7	-6.8	n.d.	n.d.	n.d.	-17.2
AG-02'-03	+28.6	+35.0	+37.3	-7.1	n.d.	n.d.	n.d.	-17.4
AG-02'-04	+24.0	+35.6	+21.5	-5.2	n.d.	n.d.	n.d.	-16.9
AG-02'-05	+24.7	+33.6	+21.5	-5.8	n.d.	n.d.	n.d.	n.d.
AG-02'-06	+28.7	+40.7	+30.0	-4.3	n.d.	n.d.	n.d.	n.d.
AG-02'-07	+42.7	+52.3	n.d.	n.d.	n.d.	n.d.	n.d.	n.d.
AG-02'-08	+41.4	+54.9	+35.5	-3.9	n.d.	n.d.	n.d.	n.d.
AG-02'-09	+19.9	+30.3	n.d.	n.d.	n.d.	n.d.	n.d.	n.d.
AG-02'-10	+28.1	+40.3	+30.4	-4.4	n.d.	n.d.	n.d.	n.d.
AG-02'-11	+38.1	+41.2	n.d.	n.d.	n.d.	n.d.	n.d.	n.d.
AG-02'-12	n.d.	n.d.	n.d.	n.d.	n.d.	n.d.	n.d.	n.d.
AG-02'-13	n.d.	n.d.	n.d.	n.d.	n.d.	n.d.	n.d.	n.d.
AG-02'-14	n.d.	n.d.	n.d.	n.d.	n.d.	n.d.	n.d.	n.d.
AG-02'-15	+53.2	+62.3	n.d.	n.d.	n.d.	n.d.	n.d.	n.d.
AG-02'-16	+48.3	+46.4	+27.1	-6.2	n.d.	n.d.	n.d.	n.d.
AG-02'-17	n.d.	n.d.	n.d.	n.d.	n.d.	n.d.	n.d.	n.d.
AG-02'-18	n.d.	n.d.	n.d.	n.d.	n.d.	n.d.	n.d.	n.d.
AG-02'-19	n.d.	n.d.	n.d.	n.d.	n.d.	n.d.	n.d.	n.d.
AG-02'-20	n.d.	n.d.	n.d.	n.d.	n.d.	n.d.	n.d.	n.d.
AG-02'-21	n.d.	n.d.	n.d.	n.d.	n.d.	n.d.	n.d.	n.d.
AG-02'-22	n.d.	n.d.	n.d.	n.d.	n.d.	n.d.	n.d.	n.d.
AG-02'-23	n.d.	n.d.	n.d.	n.d.	n.d.	n.d.	n.d.	n.d.
AG-02'-24	n.d.	n.d.	n.d.	n.d.	n.d.	n.d.	n.d.	n.d.
AG-02'-25	n.d.	n.d.	n.d.	n.d.	n.d.	n.d.	n.d.	n.d.
AG-02'-26	n.d.	n.d.	n.d.	n.d.	n.d.	n.d.	n.d.	n.d.
AG-02'-27	n.d.	n.d.	n.d.	n.d.	n.d.	n.d.	n.d.	n.d.
AG-02'-28	n.d.	n.d.	n.d.	n.d.	n.d.	n.d.	n.d.	n.d.
AG-02'-29	n.d.	n.d.	n.d.	n.d.	n.d.	n.d.	n.d.	n.d.
AG-02'-30	n.d.	n.d.	n.d.	n.d.	n.d.	n.d.	n.d.	n.d.
AG-02'-31	n.d.	n.d.	n.d.	n.d.	n.d.	n.d.	n.d.	n.d.
AG-02'-32	n.d.	n.d.	n.d.	n.d.	n.d.	n.d.	n.d.	n.d.
AG-02'-33	n.d.	n.d.	n.d.	n.d.	n.d.	n.d.	n.d.	n.d.
Input Water								
	+16.5	+21.4	n.d.	n.d.	n.d.	+10.3	+10.6	-12.6

(n.d.:not determined)

Table S6: N consumption in the column experiments

Table S6. Mass balance of nitrogen compounds in both column experiments.

CCC				
	Input (mmols)	**Output (mmols)**	**Denitrified (mmols)**	**%**
Stage I	40.5	18.0	22.5	55.5
Stage II	77	15.7	61.3	79.6
Total	117.4	33.7	83.7	71.3

PTC				
	Input (mmols)	**Output (mmols)**	**Denitrified (mmols)**	**%**
Stage I	38.6	3.0	35.6	92.2
Stage II	129.1	24.4	104.7	81.1
Total	167.7	27.4	140.3	83.7